nature medicine

© 2006 Nature Publishing Group http://www.nature.com/naturemedicine

Quantitative imaging of *Plasmodium* transmission from mosquito to mammal

Rogerio Amino[1,4], Sabine Thiberge[1], Béatrice Martin[1], Susanna Celli[2], Spencer Shorte[3], Friedrich Frischknecht[1,4] & Robert Ménard[1]

***Plasmodium*, the parasite that causes malaria, is transmitted by a mosquito into the dermis and must reach the liver before infecting erythrocytes and causing disease. We present here a quantitative, real-time analysis of the fate of parasites transmitted in a rodent system. We show that only a proportion of the parasites enter blood capillaries, whereas others are drained by lymphatics. Lymph sporozoites stop at the proximal lymph node, where most are degraded inside dendritic leucocytes, but some can partially differentiate into exoerythrocytic stages. This previously unrecognized step of the parasite life cycle could influence the immune response of the host, and may have implications for vaccination strategies against the preerythrocytic stages of the parasite.**

Plasmodium sporozoites are transmitted to a mammalian host during the bite of an infected mosquito[1,2] and are deposited in the dermis of the host[3–6]. To analyze the *in vivo* behavior of sporozoites, we used *Anopheles stephensi* mosquitoes and clones of the rodent-infecting parasite *Plasmodium berghei* that express the green fluorescent protein[7,8]. Sporozoites naturally transmitted to different rodent species were imaged by epifluorescence time-lapse microscopy.

To examine sporozoites in the dermis, we allowed a single mosquito to probe the ear pinnae of an anesthetized hairless mouse for 1 min, and observed the probed site by wide-field or confocal microscopy. In 12 such experiments, we detected an average of ~20 fluorescent sporozoites in the imaged tissue volume (**Supplementary Table 1** online). Most sporozoites in the dermis showed a robust forward-gliding locomotion that followed a tortuous and apparently random path (**Fig. 1a** and **Supplementary Movie 1** online), contrasting with the circular pattern of sporozoites gliding *in vitro* in the presence of serum[9] or with the typically back-and-forth motion of sporozoites in mosquito salivary ducts[2]. Approximately 75% of sporozoites were gliding in the dermis and *in vitro* upon observation intervals of 10 s, whereas less than 10% were moving in mosquito salivary ducts upon observation intervals of 100 s. Motile sporozoites both in the dermis and *in vitro* glided at an average speed of 1–2 μm/s, whereas sporozoites in the salivary ducts glided at only 0.1 μm/s (**Fig. 1b**). Despite their strongly induced motility, most dermis sporozoites remained in the imaged volume over time (**Fig. 1c**,**d**), owing to both their sinuous gliding path and declining average velocity (**Fig. 1e**). This allowed a quantitative assessment of the sporozoite fate in the dermis.

To image how sporozoites leave the site of mosquito bite, blood vessels were revealed by tracking the movement of erythrocytes with transmission light at high image-acquisition rates before or after imaging fluorescent sporozoites, or the blood flow was tracked by intravenous injection of fluorescent bovine serum albumin. As expected, sporozoites invaded blood vessels (**Supplementary Movie 2** online). Sporozoites gliding in the dermis interacted with blood vessel walls, frequently decreased their speed when gliding along them (**Fig. 2a** and **Supplementary Movie 2** online) and were suddenly carried away at speeds similar to that of erythrocytes in the dermal capillary bed, that is, ~40–50 μm/s (**Fig. 2a–c**). A typical blood vessel invasion process took less than 1 min, and could follow periods of sporozoite active motility or arrest along the blood vessel wall (**Fig. 2b**,**c**).

Sporozoites also invaded lymphatic vessels (**Supplementary Movie 3** online). Sporozoites gliding in the dermis with their anterior poles oriented forward were subsequently seen drifting in a sideward and low-velocity movement (**Fig. 3a–c**) along a path that did not coincide with the trajectory of a blood vessel (**Fig. 3c**). The presence of sporozoites inside lymphatic vessels was confirmed by confocal microscopy after intradermal injection of sporozoites with red fluorescent dextran (**Fig. 3d**). Furthermore, parasites were found in the first draining lymph node after inoculation in the ear (data not shown) or in the footpads of mice (**Supplementary Fig. 1** online). Based on data collected from 1-h time-lapse analysis of dermis sporozoites delivered during 12 independent mosquito bites, we estimate that in 1 h ~50% of the inoculated sporozoites leave the site of bite by invading either blood (~70%; **Fig. 2a**) or lymphatic (~30%; **Fig. 3a**) vessels (**Fig. 3e**). Unexpectedly, an important proportion of the sporozoites remained in the dermis, where some were detected up to 7 h after injection.

The traditional assumption is that sporozoites potentially drained by lymphatic vessels would eventually reach the blood and the liver[10,11]. To analyze sporozoites in the lymphatic system, 10 infected mosquitoes were allowed to bite for 1 min the footpad of anesthetized

[1]Unité de Biologie et Génétique du Paludisme, [2]Groupe Dynamique des Réponses Immunes and [3]Plate-forme d'Imagerie Dynamique, Institut Pasteur, 25-28 rue du Dr Roux, 75724 Paris cedex 15, Paris, France. [4]Present addresses: Departamento de Bioquimica, Universidade Federal de Sao Paulo, Rua Três de Maio 100, 04044-020, Sao Paulo, S.P., Brazil (R.A.); Department of Parasitology, University of Heidelberg Medical School, Im Neuenheimer Feld 324, 69120 Heidelberg, Germany (F.F.). Correspondence should be addressed to R.A. (roti@ecb.epm.br), F.F. (freddy.frischknecht@med.uni-heidelberg.de) or R.M. (rmenard@pasteur.fr).

Received 22 June 2005; accepted 29 November 2005; published online 22 January 2006; doi:10.1038/nm1350

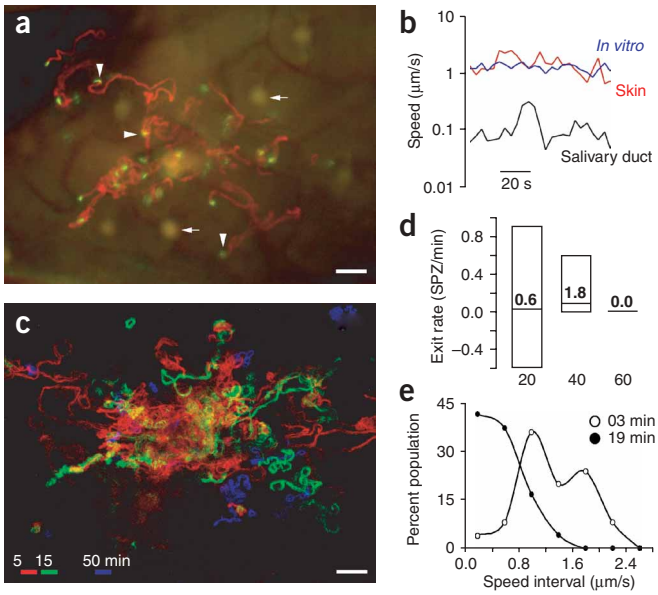

Figure 1 Sporozoite motility in the dermis. (**a**) Sporozoites injected by a single mosquito into the ear of a mouse were imaged for 200 s. The path of sporozoites is represented by a maximum-intensity projection of the fluorescent signal (red). Arrowheads indicate sporozoites (green) and arrows indicate autofluorescent patches on the skin surface. Scale bar, 50 μm. (**b**) Gliding velocity of a representative motile sporozoite in a mosquito salivary duct (black line), on a glass slide (blue line) and in the mouse dermis (red line). (**c**) Dispersion of sporozoites in the dermis, represented by maximum fluorescent intensity projections of parasites moving over 400 s at 5 min (red), 16 min (green) and 48 min (blue) after the mosquito bite. The movement of most sporozoites is localized at the site of bite and decreases over time. Scale bar, 50 μm. (**d**) Number of sporozoites (SPZ) that leave the microscope field per minute by gliding motility (exit rate). Bars represent the range of the exit rates, lines the average exit rate and numbers above the lines the average number of sporozoites that left the field in the considered 20-min interval ('20', '40' and '60' refer to the 0–20-min, 20–40-min and 40–60-min intervals, respectively). Negative values indicate sporozoites entering the field. (**e**) Distribution of the individual average velocity of sporozoites in the dermis. The open and filled circles represent sporozoites examined at 3 and 19 min after a single mosquito bite, respectively.

hairless mice. At 1 h, 2 h and 4 h after bite, we dissected the proximal (popliteal) and distal (iliac) draining lymph nodes and determined the number of fluorescent sporozoites. We found an average of ~50 parasites in the popliteal node at the various times after bite (**Fig. 4a**), which represent ~25% of the inoculated sporozoites, assuming that ~20 sporozoites are delivered by each mosquito. In the iliac node, however, sporozoites were only exceptionally encountered up to 4 h after bite (**Fig. 4a**). To test whether some lymph sporozoites could nonetheless reach the blood circulation through the thoracic duct, the latter was cannulated in mice that were subsequently infected as above. In three experiments, we could not detect sporozoites in the lymph collected for 3 h after bite (~2 ml). We carried out similar experiments with C57/Bl6 mice and in Brown-Norway rats, which are both highly permissive to *P. berghei*. Again, only a very small proportion (<1%) of sporozoites were found beyond the popliteal lymph node, confirming that most of the sporozoites drained by lymphatic vessels stopped their journey in the proximal lymph node. We also found that a ~20-fold higher proportion of sporozoites reached the popliteal node when sporozoites were injected by mosquitoes than intradermally with a syringe, and that sporozoites need to be motile to gain access to the lymphatic system (**Supplementary Fig. 1** online).

We assessed the fate of sporozoites in the popliteal lymph nodes by imaging sporozoites in isolated lymph nodes and by labeling with antibodies after fixation. The proportion of gliding sporozoites in the popliteal node was high at early time points (~60% at 1 h), and, like in the skin, decreased with time (~20% at 2 h). Early after injection (1–2 h), we found sporozoites mainly in the subcapsular zone of the lymph nodes close to the afferent lymph vessel and subcapsular sinuses, but they relocalized toward the efferent vessel over time. In the process, the proportion of parasites showing a normal shape sharply declined (**Fig. 4b**). Whereas at 1 h most parasites had the characteristic sporozoite shape, at 4 h most parasites appeared damaged with diffuse red circumsporozoite protein–specific fluorescence, and at 8 h most fluorescence had disappeared. To examine whether parasites interacted with lymph node dendritic

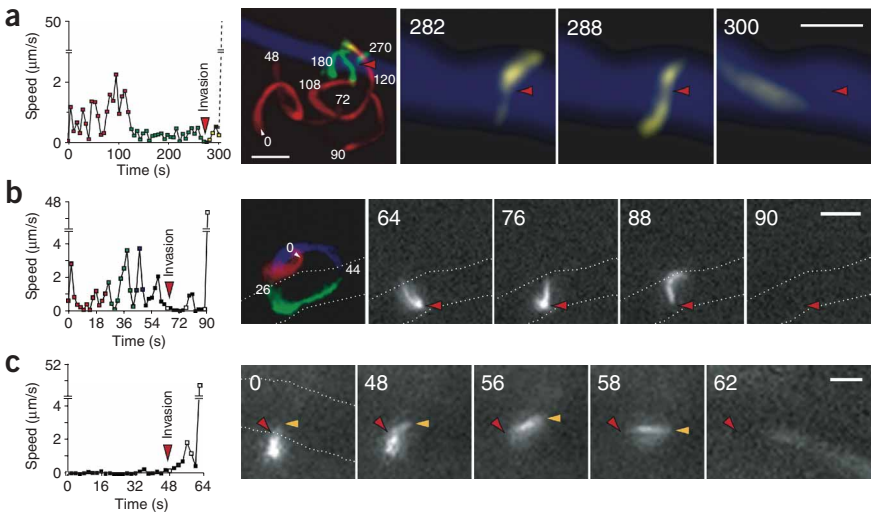

Figure 2 Dermis sporozoites invade blood vessels. (**a–c**) Each panel shows the velocity profile (left) of the sporozoite analyzed by time-lapse microscopy (right). Scale bars, 10 μm. (**a**) The maximum-intensity projection (left, numbers indicate the sporozoite position at various times in seconds) shows a sporozoite gliding in the dermis (red; 20 confocal images over 120 s), decreasing its speed as it glides along the blood vessel wall (green; 25 confocal images over 150 s) and moving through the vessel wall (yellow). The blood vessel tracked by fluorescent BSA is depicted in blue. The single time frames on the right (time in seconds indicated) show the sporozoite invading the vessel wall. The arrowheads indicate the site of sporozoite invasion. (**b**) The maximum projection (left image) shows a sporozoite gliding in the vicinity of a blood vessel. The single time frames on the right show the sporozoite entering the vessel. The dotted lines outline the blood vessel. (**c**) The single time frames on the right show a sporozoite invading a blood vessel and being transported away with the blood. This parasite rests before entering the vessel. The red arrowheads indicate the vessel wall and the yellow arrowheads indicate the tip of the sporozoite.

© 2006 Nature Publishing Group http://www.nature.com/naturemedicine

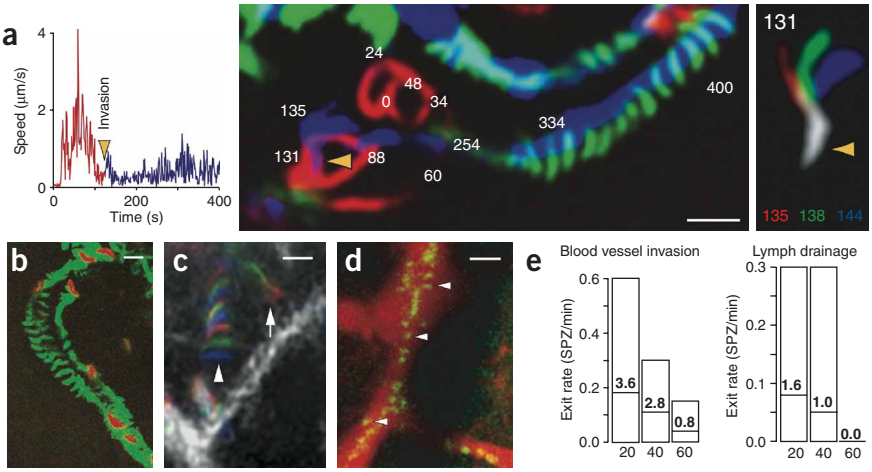

Figure 3 Dermis sporozoites invade lymphatic vessels. (**a**) The panel shows the velocity profile (left) of the sporozoite analyzed by spinning-disk confocal time-lapse microscopy (right). The maximum-intensity projection (left; numbers indicate the sporozoite position at various times in seconds) shows a sporozoite gliding in the dermis (red) and drifting passively (blue; the green projection shows other sporozoites drifting along the same trajectory 20 min later). The panel on the right (time in seconds indicated) shows the sporozoite drifting laterally after invasion of the vessel. The arrowheads indicate the site of sporozoite invasion. Scale bar, 10 μm. (**b**) Maximum-intensity projection of several sporozoites (red, $t = 0$ s) drifting laterally along the same trajectory (green, 52 frames spanning 400 s). Scale bar, 10 μm. (**c**) The path of a sporozoite that drifts laterally (arrowhead; blue: 0 s, 6 s and 12 s; green: 2 s, 8 s and 14 s; red: 4 s, 10 s and 16 s) differs from that of a sporozoite gliding with its anterior pole oriented forward (arrow) and does not coincide with the trajectory of a blood vessel, shown in white. Scale bar, 10 μm. (**d**) Overlay of confocal images (14 frames spanning 70 s) after intradermal injection of fluorescent dextran (red), which is drained by lymphatics, and of sporozoites (green) shows the colocalization of sporozoites and dextran. Scale bar, 50 μm. (**e**) Number of sporozoites that leave the microscope field per minute by invading blood or lymphatic vessels (exit rate). Bars represent the range of the exit rates, lines the average exit rate and numbers above the lines the average number of sporozoites (SPZ) that left the field in the considered 20-min interval ('20', '40' and '60' refer to the 0–20-min, 20–40-min and 40–60-min intervals, respectively).

cells (DCs), we stained lymph nodes with antibodies to CD11c, a DC-specific marker. At 2 h and 4 h after bite, ~20% and ~50% of the lymph node parasites were closely associated with DCs, respectively. Sporozoites were either extracellular, with the surface areas of the two cells apposed, or were detected inside DCs as normally shaped or partially degraded parasites (**Fig. 4c**).

We then tested whether *P. berghei* sporozoites could mature into exoerythrocytic forms (EEFs) inside lymph nodes. Normal development of *P. berghei* inside rodent hepatocytes takes ~52 h, and consists of a remodeling process from the elongated sporozoite to an enlarged and spherical EEF, in which nuclei divide and from which daughter cells eventually bud off[12]. To investigate parasite development in the lymph nodes, we subjected the footpads of C57/Bl6 mice to 15 mosquito bites or to intradermal injection of 10^5 salivary gland sporozoites, and sought fluorescent parasites in the popliteal lymph node and in the liver at 15 h, 24 h and 52 h after injection. After delivery by mosquito or syringe, we detected a small proportion of fluorescent parasites in the lymph node at 15 h and 24 h (**Fig. 4d**). To investigate the location of these parasites, we stained lymph nodes with antibodies to the following: CD11c; CD11b, a

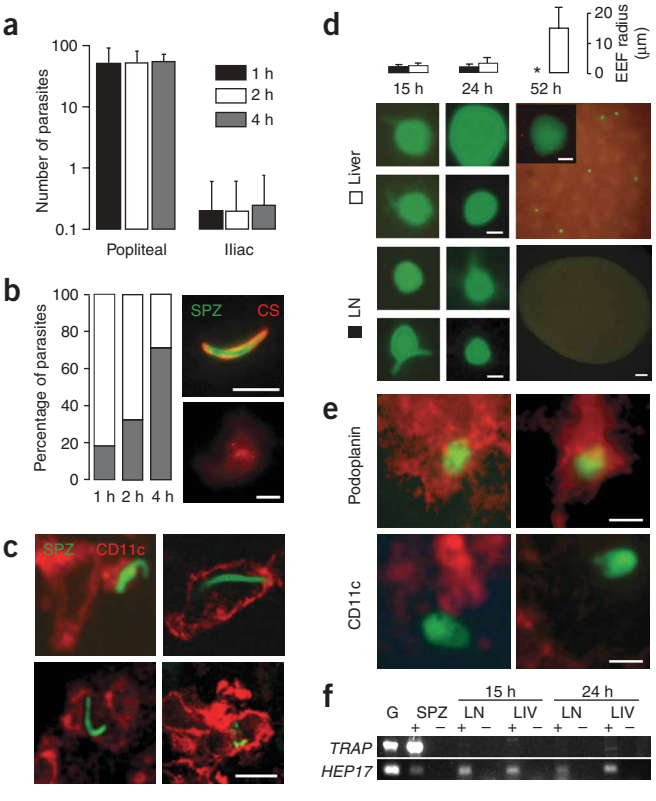

Figure 4 Sporozoite fate in the draining lymph node. (**a**) Parasite quantification in the popliteal and iliac lymph nodes at 1 h, 2 h or 4 h after sporozoite delivery in the footpad of mice by 10 mosquitoes. (**b**) Percentage of parasites at different times after injection that show the usual banana-like shape (white portion of bar) or altered shapes (gray portion of bar). Representative parasites labeled with GFP (green) and antibodies to the circumsporozoite protein (CS, red) with normal or altered shapes are shown in upper and lower images on the right, respectively. Scale bars, 10 μm. (**c**) Lymph node sporozoites (green) interact with DCs labeled with antibodies to CD11c (red) 4 h after injection. (**d**) Parasite differentiation in the draining popliteal lymph node (LN) and in the liver at 15 h, 24 h and 52 h after injection of sporozoites in the mouse footpads. The average radius of EEFs in the lymph node (black bars) and in the liver (white bars) are indicated. The upper and lower images on the left show EEFs developing at the corresponding time points in the liver and in the lymph node, respectively. Scale bars, 2 μm. The images on the right show the presence (liver) or absence (lymph node) of EEFs at 52 h. Scale bars are 100 μm and 10 μm (inset), respectively. (**e**) Lymph node EEFs (green) colocalize with endothelial cells labeled with antibodies to podoplanin (red, upper images), but not with DCs labeled with antibodies to CD11c (red, lower images), 24 h after injection. (**f**) Development of lymph node sporozoites into EEFs is shown by RT-PCR analysis of the parasite genes *TRAP* and *HEP17*. Samples include the genomic DNA of the parasite (G), RNA from sporozoites collected from mosquito salivary glands (SPZ), lymph node EEFs (LN) or liver EEFs (LIV) at indicated times after injection; + and – indicate presence or absence of reverse transcriptase, respectively.

© 2006 Nature Publishing Group http://www.nature.com/naturemedicine

macrophage-monocyte marker; CD45, a generic leukocyte antigen; and podoplanin, which is specifically expressed by lymphatic but not blood vascular endothelial cells. Parasites colocalized only with podoplanin-positive cells (**Fig. 4e**), suggesting that lymph node EEFs associate with endothelial but not hematopoietic cells. Although at 15 h lymph node parasites had a size, shape and fluorescence intensity that were similar to those of EEFs developing inside hepatocytes of the same mice, at 24 h the lymph node parasites had a smaller size than that of concomitant liver EEFs (**Fig. 4d**). At 52 h after injection, fluorescence was not detected in popliteal nodes, whereas large fluorescent EEFs were present in the liver (**Fig. 4d**). To confirm that parasites could indeed partially develop inside lymph nodes, we used RT-PCR (**Fig. 4f**) to assess expression of *TRAP*, which normally peaks in sporozoites and decreases in liver EEFs[13,14], and of *HEP17*, which is weak in sporozoites and sharply increases in liver EEFs[15]. Expression of *HEP17* was detected in lymph node EEFs at both 15 and 24 h, whereas expression of *TRAP* was not, showing the presence of developing parasites inside lymph nodes.

In conclusion, the *Plasmodium* sporozoites inoculated by *Anopheles* mosquitoes seem to have various fates in the mammalian host. Sporozoites can either remain in the dermis, after exhaustion of their motility, or invade blood or lymphatic vessels. Sporozoites drained by lymphatics are trapped in the proximal lymph node, where most are degraded but some can partially develop and deliver early EEF antigens. In view of the renewed interest in vaccination against preerythrocytic stages of the parasite using live attenuated sporozoites[16–20], it will be important to investigate the contribution of lymph node parasites in mounting a protective immune response, or instead in inducing tolerance to parasite antigens. The increasingly powerful imaging tools, particularly in the field of immunoimaging[21–23], should help in dissecting these new host-parasite interactions and the host responses they generate in a physiological context.

METHODS

Parasites. We used the *P. berghei* NK65 clone expressing the green fluorescent protein (GFP) from the stage-specific circumsporozoite protein promoter[7], which yields maximum fluorescence at the sporozoite stage, as well as the *P. berghei* ANKA clone expressing GFP from the EF-1alpha promoter[8], which yields fluorescence throughout the parasite life cycle including in EEFs.

Mosquitoes. *A. stephensi* (Sda500 strain) mosquitoes were reared at the Center for Production and Infection of *Anopheles* (CEPIA) of the Pasteur Institute using standard procedures. Mosquitoes were fed on *P. berghei*–harboring mice (parasitemia >1%) 3–5 d after emergence, kept at elevated humidity (70%) in dedicated incubators or rooms at 21°C and fed on 10% sucrose solution. Mosquitoes were kept in the absence of sucrose for 1 d before the gametocyte-harboring feed and received a blood meal from an uninfected mouse usually 1 week after the infectious blood meal. We isolated sporozoites from sporozoite-positive salivary glands 15–22 d after the infectious blood meal (post blood meal, p.b.m.). We dissected infected salivary glands and kept them on ice in PBS, or in tissue culture medium with or without 5% FCS. Infected mosquitoes used for transmission experiments (days 18–22 p.b.m.) were deprived of sucrose for 1–4 d before experimentation, which enhanced the bite rate of mosquitoes.

Rodent infection by mosquito bites. We anesthetized (ketamine-xylazine) C57Bl/6 (Janvier) or SKH1-hairless (Charles River) mice or Brown Norway rats (Janvier) and held them with an ear or a footpad over a small gauze-covered beaker containing 10 mosquitoes. For imaging in the ear, a mosquito was allowed to probe for 1 min before the rodent was removed. We scanned the site of bite against a bright lamp to localize the hematoma and placed the rodent on the motorized table of an inverted microscope (Zeiss Axiovert 200 or Olympus IX71). For sporozoite analysis in lymph nodes, 10 mosquitoes were allowed to bite for 1 min each the footpad of an anesthetized rodent. We removed lymph nodes by minimally invasive surgery after 1 h, the rodent being kept asleep, or at later times, the rodent being allowed to wake up and then being anesthetized again for operation. We injected rodents with 3 µl of salivary gland sporozoites intradermally with a modified Hamilton microsyringe (World Precision Instruments). During *in vivo* imaging, animals were heated with a homothermic blanket system (Harvard Apparatus).

Mouse manipulations. For visualizing the lymphatic vessels, we microinjected (Nanojet, Drummond Scientific) fluorescent dextran (Sigma, Molecular Probes) intradermally into mice at a concentration of 1 mg/ml. For labeling the blood circulation, we injected fluorescent BSA or high-molecular-weight dextran (Molecular Probes) intravenously (5 µl) or intraperitoneally (150 µl) into mice at a concentration of 10 mg/ml.

To test the presence of sporozoites in the general lymphatic circulation, we anesthetized rodents with Avertin (2,2,2-tribromo-ethanol Fluka AG, CH, in amyl-alcohol, Sigma; 0.1 ml/10 g body weight), made a lateral left abdominal incision and exposed the retroperitoneal area, cannulated the thoracic duct (polythene tubing (inner diameter, 40 mm; outer diameter, 80 mm), Portex Limited) and collected the lymph over 3 h in an Eppendorf tube after closure of the abdominal wall in two layers. All experiments using rodents were approved by the committee of our institute and were performed in accordance with the applicable guidelines and regulations.

Microscopy and image analysis. We carried out microscopic analysis using inverted Zeiss or Olympus microscopes with the rodent resting on a heated platform. Images were captured using a Perkin Elmer UltraView spinning disk confocal microscope, a TILL vision workstation or the Olympus Cell R software package with 5–40× long-distance dry or oil-immersion objectives (Zeiss, Olympus) occasionally magnified with a 1.6× Optovar. Image acquisition times varied between 20 ms and 2 s depending on tissue depth and microscopy set up. We recorded continuous single movies for up to 25 min. Image files were processed using ImageJ. We performed automated or manual tracking with the ImageJ Multitracker PlugIn (from N. Stuurman, University of California, San Francisco) or the manual tracking tool and compiled data in Microsoft Excel. When images were recorded in multiple z-layers, those were projected into a single layer and the resulting two-dimensional data set was analyzed. We washed isolated popliteal and iliac lymph nodes and placed them in PBS or medium on glass-bottom dishes (MatTek) and photographed them with a Nikon SMZ 1500 fluorescent stereomicroscope and a Nikon Coolpix, or imaged them using the Olympus IX71 or Perkin Elmer UtlraView microscopes. Images were processed and assembled using the ImageJ and Adobe software package. All graphs show mean ± s.d.

RT-PCR analysis. To assess gene expression of the parasite inside lymph nodes and liver, we intradermally injected salivary gland sporozoites into the footpad of mice, and at various times after injection removed the popliteal lymph node and the liver, extracted total RNA and treated it with DNAse I, synthesized cDNA using reverse transcription from 1 µg of total RNA, and carried out PCR amplification using oligonucleotide primers specific for the *TRAP* and *HEP17 P. berghei* genes using the following protocol: 94 °C for 3 min, 40 cycles of 94 °C for 30 s, 55 °C for 30 s and 72 °C for 1 min, and 72 °C for 3 min. For sporozoites, we carried out RT-PCR from total RNA extracted from 10 infected salivary glands ($\sim 10^5$ sporozoites).

Note: Supplementary information is available on the Nature Medicine website.

ACKNOWLEDGMENTS

We thank A. Genovesio, C. Zimmer and J.-C. Olivo-Marin for help with tracking analysis, P. Roux for help with confocal microscopy, the members of the Center for Production and Infection of *Anopheles* of the Pasteur Institute for mosquitoes rearing, B. Boisson for help in RT-PCR and C. Janse for providing PbGFPCON parasites. We are grateful to G. Milon, C. Bourgouin, P. Sinnis, S. Mecheri and F. Zavala for comments on the manuscript. The work was supported by funds from the Pasteur Institute (Strategic project 'Grand Programme Horizontal *Anopheles*'), the Howard Hughes Medical Institute and the European Commission (FP6 BioMalPar Network of Excellence). R.A. was supported by the Pasteur Institute Grand Programme Horizontal fellowship and F.F. by a Human Frontier Science Program long-term fellowship. R.M. is a Howard Hughes Medical Institute International Scholar.

© 2006 Nature Publishing Group http://www.nature.com/naturemedicine

COMPETING INTERESTS STATEMENT
The authors declare that they have no competing financial interests.

Published online at http://www.nature.com/naturemedicine/
Reprints and permissions information is available online at http://npg.nature.com/reprintsandpermissions/

1. Beier, J.C. Malaria parasite development in mosquitoes. *Annu. Rev. Entomol.* **43**, 519–543 (1998).
2. Frischknecht, F. *et al.* Imaging movement of malaria parasites during transmission by *Anopheles* mosquitoes. *Cell. Microbiol.* **6**, 687–694 (2004).
3. Boyd, M.F. & Kitchen, S.F. The demonstration of sporozoites in human tissues. *Am. J. Trop. Med. Hyg.* **19**, 27–31 (1939).
4. Ponnudurai, T., Lensen, A.H., van Gemert, G.J., Bolmer, M.G. & Meuwissen, J.H. Feeding behaviour and sporozoite ejection by infected *Anopheles stephensi*. *Trans. R. Soc. Trop. Med. Hyg.* **85**, 175–180 (1991).
5. Matsuoka, H., Yoshida, S., Hirai, M. & Ishii, A. A rodent malaria, *Plasmodium berghei*, is experimentally transmitted to mice by merely probing of infective mosquito, *Anopheles stephensi*. *Parasitol. Int.* **51**, 17–23 (2002).
6. Sidjanski, S. & Vanderberg, J.P. Delayed migration of *Plasmodium* sporozoites from the mosquito bite site to the blood. *Am. J. Trop. Med. Hyg.* **57**, 426–429 (1997).
7. Natarajan, R. *et al.* Fluorescent *Plasmodium berghei* sporozoites and pre-erythrocytic stages: a new tool to study mosquito and mammalian host interactions with malaria parasites. *Cell. Microbiol.* **3**, 371–379 (2001).
8. Franke-Fayard, B. *et al.* A *Plasmodium berghei* reference line that constitutively expresses GFP at a high level throughout the complete life cycle. *Mol. Biochem. Parasitol.* **137**, 23–33 (2004).
9. Vanderberg, J.P. Studies on the motility of *Plasmodium* sporozoites. *J. Protozool.* **21**, 527–537 (1974).
10. Vaughan, J.A., Scheller, L.F., Wirtz, R.A. & Azad, A.F. Infectivity of *Plasmodium berghei* sporozoites delivered by intravenous inoculation versus mosquito bite: implications for sporozoite vaccine trials. *Infect. Immun.* **67**, 4285–4289 (1999).
11. Krettli, A.U. & Dantas, L.A. Which routes do *Plasmodium* sporozoites use for successful infections of vertebrates? *Infect. Immun.* **68**, 3064–3065 (2000).
12. Meis, J.F. & Verhave, J.P. Exoerythrocytic development of malaria parasites. *Adv. Parasitol.* **27**, 1–61 (1988).
13. Grüner, A.C. *et al.* Insights into the *P. y. yoelii* hepatic stage transcriptome reveal complex transcriptional patterns. *Mol. Biochem. Parasitol.* **142**, 184–192 (2005).
14. Sacci, J.B., Jr. *et al.* Transcriptional analysis of *in vivo Plasmodium yoelii* liver stage gene expression. *Mol. Biochem. Parasitol.* **142**, 177–183 (2005).
15. Charoenvit, Y. *et al. Plasmodium yoelii*: 17-kDa hepatic and erythrocytic stage protein is the target of an inhibitory monoclonal antibody. *Exp. Parasitol.* **80**, 419–429 (1995).
16. Luke, T.C. & Hoffman, S.L. Rationale and plans for developing a non-replicating, metabolically active, radiation-attenuated *Plasmodium falciparum* sporozoite vaccine. *J. Exp. Biol.* **206**, 3803–3808 (2003).
17. Mueller, A.K., Labaied, M., Kappe, S.H. & Matuschewski, K. Genetically modified *Plasmodium* parasites as a protective experimental malaria vaccine. *Nature* **433**, 164–167 (2005).
18. Mueller, A.K. *et al. Plasmodium* liver stage developmental arrest by depletion of a protein at the parasite-host interface. *Proc. Natl. Acad. Sci. USA* **102**, 3022–3027 (2005).
19. Good, M.F. Genetically modified *Plasmodium* highlights the potential of whole parasite vaccine strategies. *Trends Immunol.* **26**, 295–297 (2005).
20. Tongren, J.E., Zavala, F., Roos, D.S. & Riley, E.M. Malaria vaccines: if at first you don't succeed…. *Trends Parasitol.* **20**, 604–610 (2004).
21. Bousso, P. & Robey, E. Dynamics of $CD8^+$ T cell priming by dendritic cells in intact lymph nodes. *Nat. Immunol.* **4**, 579–585 (2003).
22. Hugues, S. *et al.* Distinct T cell dynamics in lymph nodes during the induction of tolerance and immunity. *Nat. Immunol.* **5**, 1235–1242 (2004).
23. Sumen, C., Mempel, T.R., Mazo, I.B. & von Andrian, U.H. Intravital microscopy: visualizing immunity in context. *Immunity* **21**, 315–329 (2004).

© 2006 Nature Publishing Group http://www.nature.com/naturemedicine